Characterization of Aged Li-Ion Battery Components for Direct Recycling Process Design

Kae Fink,* Shriram Santhanagopalan,,z Julia Hartig, and Lei Cao**

National Renewable Energy Laboratory, Golden, Colorado 80401, USA

Novel nondestructive recycling methods for lithium ion batteries (LIBs) are under investigation but lack the process engineering specifications required for full-scale operation. Specifically, the ability of end-of-life LIB components to withstand the stresses inherent in industrial manufacturing techniques has not been established. In this paper, we mechanically characterize the electrodes of both fresh and "cycle-aged" (C-A) cells, and couple this with electrochemical analysis to establish reprocessing requirements in the context of roll-to-roll (R2R) direct recycling. Cycle-aging is found to significantly reduce the tensile strength of electrodes and C-A cathodes reach elastic deformation at a lower strain than do fresh cathodes. This implies that both roll tension and calendering force may need to be reduced for C-A components relative to fresh components to avoid irreversible damage. Electrochemical analysis suggests that phase change and buildup of electrolyte residues at both the primary particle and in the inter-particle pore space may contribute to cathode degradation. The combination of these mechanical and electrochemical findings is crucial to informing the process design of industrial-scale nondestructive LIB recycling methods.

 [DOI: 10.1149/2.0781915jes]

Manuscript submitted August 14, 2019; revised manuscript received October 20, 2019. Published November 14, 2019.

In the past decade, increased reliance on high-powered electronics has led to unprecedented growth in the manufacture and dissemination of lithium-ion batteries (LIBs). The ubiquity of LIBs across all sectors of society, from personal electronics to grid-scale storage solutions, has fueled a nearly $31.2 billion global LIB market – a value that is expected to double in the next four years.[1] In particular, increased adoption of electric vehicles (EVs) is predicted to drive an exponential increase in LIB demand, from 19 GWh globally in 2015 to 1,293 GWh forecasted by 2030.[2] This surge in demand has placed significant stress on the material supply chain for LIB manufacture. Additionally, an estimated 28.5 million LIB units within the US will reach their end of life by 2029;[3] as such, there are growing environmental concerns regarding LIB disposal.

Recycling of used LIBs has been identified both as a means to stabilize the LIB supply chain and as an end-of-life solution.[4–8] There are currently three major recycling approaches under exploration: pyrometallurgical, hydrometallurgical, and direct. Pyrometallurgical recycling is the most mature battery recycling process,[9,10] and seeks to break down components (i.e., anode, cathode, separator) and external packaging into elemental form before reprocessing them back into usable molecules.[9] This method allows for significant recovery of Co, Ni, and Cu and enables the simultaneous processing of mixed electrode chemistries, but is expensive and highly energy intensive, and thus may be economically unfeasible.[7–9]

Hydrometallurgial recycling – the dominant LIB recycling method in both China and Korea[11,12] – consists of breaking down components into molecular compounds, which can be further processed to regenerate usable LIB material.[8,9] Within the US, optimizing and improving the scalability of hydrometallurgical recycling is an area of active research.[13–21] While hydrometallurgical recycling generally yields a higher-value product stream and is less energy-intensive than pyrometallurgial recycling, there are still significant drawbacks to this approach. The use of chemical treatment to recover active materials from the cells adds cost to the recycling process, and also necessitates wastewater treatment procedures.[9]

The final recycling approach is direct recycling, whereby whole cells and/or components are recovered in essentially intact form, and are then remediated (chemically and/or physically) to reconstruct usable cells.[8,9,22] The feasibility of recovering electrode capacity though re-lithiation has already been demonstrated,[23–29] and preliminary work has suggested that reconditioned electrodes can be analytically indistinguishable from fresh electrodes.[22] To date, all known work with direct recycling has been done at the laboratory scale;[8,26–32] as such, comprehensive process engineering optimization has yet to be performed to make this approach viable on an industrial scale.

Unlike pyrometallurgial and hydrometallurgical techniques, direct recycling does not require mechanical destruction of LIB components. We propose that, to maximize efficiency and cost-effectiveness, component integrity should be maintained throughout the reconditioning process. Under such a method, "aged" components (i.e., those from end-of-life LIBs) would be reprocessed and calendered in a manner similar to fresh components, thereby avoiding the milling, shredding, and separation steps currently employed in other recycling methods.[8,22]

The feasibility of an industrial-scale direct recycling process depends on the mechanical strength of the components comprising the recycling feedstock. In a typical electrode manufacturing process, active material and binder are mixed in either a batch mixer or a continuous dispersion mixing device and the resulting slurry is then coated onto rolls of collector foils as the foils continuously move on a winding belt. Following oven drying to evaporate solvent, the coated electrodes are calendared and then re-wound into cylindrical cells. Such roll-to-roll (R2R) manufacturing allows for high throughput and minimizes waste relative to other coating technologies,[33,34] but must be tightly controlled at each step by parameters such as velocity, tension, and temperature.[34] The specific values of these parameters vary greatly by manufacturer,[13] but are bounded by the material properties of the feedstock and the resulting product. While it is possible that existing equipment and facilities may be repurposed to handle recycled materials, the ability of recycling feedstocks to withstand the mechanical stresses induced during R2R processing has not been established. Thus, a comprehensive characterization of the mechanical properties of aged components is essential to the design of nondestructive direct recycling methods.

Mechanical characterization methods for LIB components have already been developed and repeatedly utilized to analyze fresh components. Lai et al. have developed a mechanical model for battery modules by studying individual components, and report minimal contribution of electrode active material to overall electrode tensile strength.[35] Studies from Cannarella et al. evaluating the mechanical properties of the separator under applied stress suggest a high strain rate dependence and significant anisotropy,[36] findings that have been confirmed by several other groups.[37–40] Sahraei et al. have conducted extensive tensile tests on both electrodes and representative multilayer samples; both tensile strength and fracture strain are found to be significantly larger in anodes than in cathodes.[40] Jiang et al. have investigated the effect of coating on the mechanical performance of electrode materials, suggesting that coated electrodes have higher

*Electrochemical Society Student Member.
**Electrochemical Society Member.
zE-mail: Shriram.Santhanagopalan@nrel.gov

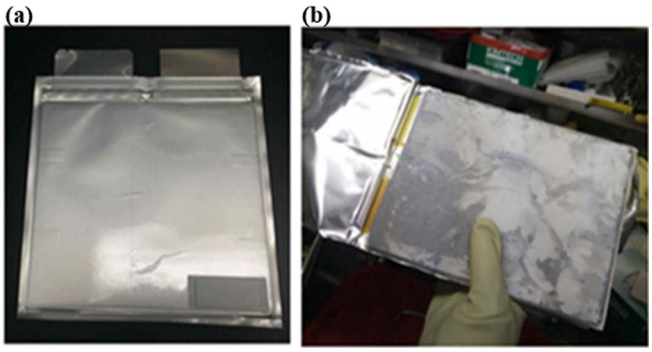

Figure 1. (a) Intact and (b) disassembled 40 Ah NMC/graphite pouch cells used in this analysis. From Zhang et al. (2017).[34]

ultimate strength and higher elongation as compared to bare current collectors.[38]

Conducting the same mechanical tests used to probe and model fresh LIB components on aged LIB components is a crucial first step in designing large-scale direct recycling methods because aging is known to degrade components differently and to varying degrees. Under conditions of repeated cycling, Al sheets (i.e., cathode current collectors) are vulnerable to localized corrosion, while Cu sheets (anode current collectors) are vulnerable to environmentally-assisted cracking.[41] Cathode aging is primarily driven by the repeated process of Li intercalation and extraction which can weaken the active material matrix.[42] This can be exacerbated by phase transitions occurring within the active material during cycling, particularly at extreme temperatures.[43] Anode aging is often characterized by Li plating which can take the form of dendrites or other surface irregularities.[42] While aging effects are highly cell- and application-specific, our previous research has suggested that anode degradation is more serious than cathode degradation under repeated cycling (2C charging rate, 1C discharging rate) at room temperature.[44,45]

Finally, in addition to these mechanical properties, the chemical, structural, and electrochemical state of aged LIB components should be used to inform the design of direct recycling processes. By understanding the various degradation modes contributing to the overall loss of cell capacity, specific remediation techniques can be developed and specifically tailored to recondition these materials.

In this paper, we seek to probe the mechanical and electrochemical properties of aged LIB components as a baseline for the development of an industrial-scale direct recycling process. Specifically, we study the combined effects of cycling and calendar aging on component response to tensile and compressive stresses. The influence of tensile strain rate and electrode coating on both fresh and aged cells is explored, and experimental data is then incorporated into our existing constitutive models. Additionally, we investigate the contribution of each aged component on the cell's overall cycling performance. Based on electrochemical analysis, we suggest several dominant degradation mechanisms associated with cathode cycle-aging. In conjunction with previous reports by our group,[33,34] this work helps to comprehensively describe the progressive aging process and resulting mechanical strength of LIB materials. By determining the ability of components to withstand the stresses that would be encountered in reconstitutive processing, we ultimately aim to: 1) determine the feasibility of non-destructive direct recycling for each component; 2) develop guidelines for the testing and sorting of recycling feedstocks; and 3) use these findings to direct the design of an industrial-scale direct recycling process.

Experimental

Sample preparation.—All samples were prepared from disassembled commercial 40 Ah NMC/graphite pouch cells containing 34 pairs of electrodes and 68 layers of separator (Fig. 1). In this analysis, fresh cells were stored under inert conditions for approximately one year. "Cycle-aged" (C-A) cells were first cycled at room temperature (~25°C) within a voltage window of 3.0–4.1 V (2C charging rate; 1C discharging rate) for 5600 cycles, then stored under argon for approximately one year and processed under atmospheric conditions for a subsequent ~1 month. Sheets of aluminum and copper current collector foils (MTI) were used without modification. Component chemistries and thicknesses are summarized in Table I.

Table I. Material chemistry and thicknesses of cell components utilized in this study.

Component	Material Chemistry	Thickness (μm)[a]
Anode (2-sided), fresh	Copper, graphite	131
Anode (2-sided), C-A	Copper, graphite	150
Anode current collector	Copper	12.5
Cathode (2-sided), fresh	Aluminum, NMC	109
Cathode (2-sided), C-A	Aluminum, NMC	175
Cathode current collector	Aluminum	16

[a]To account for sample variability, reported thicknesses represent an average of at least 6 individual measurements.

Tensile tests.—For tensile tests, cell components were cut using a paper trimmer into rectangular samples (101.6 mm (4 in) × 10.16 mm (0.4 in)). Tests were performed using an Instron 5966 Dual Column Testing System (10kN maximum load) at the National Renewable Energy Laboratory. Samples were mounted on Instron soft grips with gripping area wrapped in paper tape to minimize sample slippage. The presence of tape improved sample repeatability but did not quantitatively change tensile results. In-plane alignment of samples with the Instron clamps was visually ensured.

Each uniaxial tensile test was performed at a constant, quasi-static strain rate (0.0001 s^{-1}, 0.001 s^{-1}, or 0.01 s^{-1}) following a 1 N pre-load (applied at 0.5 mm min^{-1}). A minimum of six replicates were tested per component at each strain rate.

Previous tensile test data from this laboratory is also included for comparison. This data was obtained from cycled components (cycling conditions as described above, but not calendar-aged) that were prepared identically to the samples in this analysis. The tensile strain rate for cycled components was 0.00082 s^{-1}.

Compression tests.—For compression tests, cell components were punched into circles with diameter of 12.7 mm (0.5 in) using a hollow punch. Electrodes and current collectors were analyzed in stacks of 38 circular pieces, representing the typical number of electrode layers found in a commercial LIB pouch cell. All compression tests were conducted at a constant rate of 0.2 mm min^{-1} following a 10 N pre-load (applied at 0.4 mm min^{-1}).

Electrochemical analysis.—A variety of coin cells were assembled at room temperature in a glovebox following overnight electrode drying at 90°C. Full cells were constructed using combinations of fresh and C-A components (anode, cathode, and separator). Half cells were constructed using either fresh or C-A cathodes, fresh separator, and Li foil (MTI). In all cells, 60 mL of $LiPF_6$ in EC/DEC/DMC (1:1:1 by volume; MTI) was used as electrolyte. Following 6 h of rest at room temperature, cells were cycled at room temperature between 4.2 and 2.8 V using a multichannel cycler (Arbin). Charge/discharge rate was C/20 (0.1 mA) for the initial three cycles, and C/3 (~0.8 mA) for a subsequent 100 cycles.

Results and Discussion

Tensile tests.—The degree of tensile stress that end-of-life LIB components are able to withstand directly determines the maximum

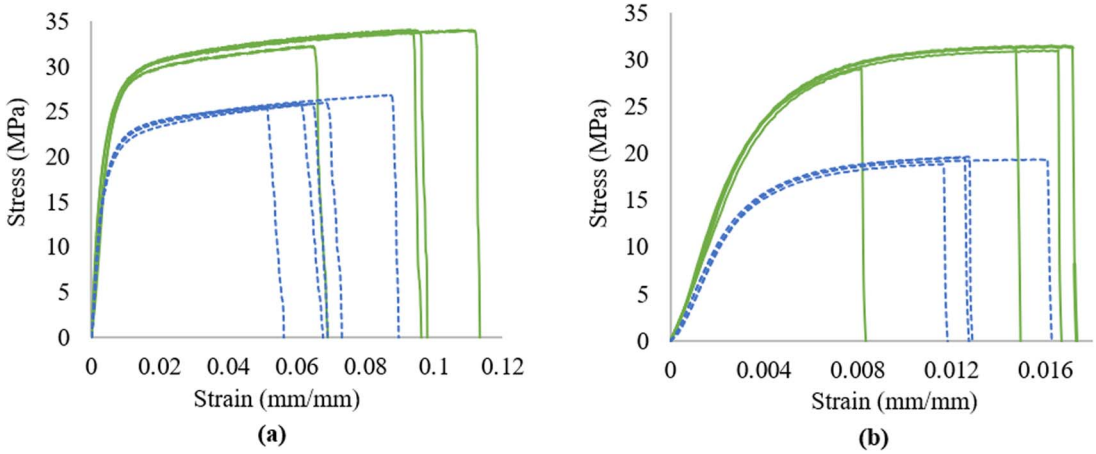

Figure 2. Experimental tensile stress-strain response for (a) anode and (b) cathode at a strain rate of 0.001 s^{-1}. Solid green lines indicate fresh samples; blue dashes indicate C-A samples. All samples demonstrate elastic-plastic behavior, with an initial elastic (linear) region shifting to a region of plastic deformation (curved). Material failure is indicated by the sharp drop to zero stress.

allowable tension for a roll-to-roll direct recycling process. Fig. 2 shows the tensile response of electrodes from both fresh and C-A cells at a strain rate of 0.001 s^{-1}. A significant decrease in both yield stress (i.e., onset of plastic deformation; mathematically described by σ^y as detailed below) and ultimate strength (i.e., material failure) with cycle-aging is observed for all components. This trend holds across all strain rates tested (see Fig. S1-S2). While sample replicates tend to show strong repeatability in terms of the initial linear region and the ultimate failure stress, there is significant variability in ultimate failure strain; this is consistent with previous reports.[35,44–46]

To quantify these observed trends, electrode stress-strain curves have been mathematically modeled. As evidenced by the shape of the curves in Figure 2, coated electrodes (cathode and anode) express elastic-plastic tensile behavior; bare current collectors (Al and Cu foils) behave similarly. Thus, Zhang et al.[46] have suggested that the behavior of electrodes and current collectors can be approximated by an isotropic linear-hardening elastic-plastic model:

$$\sigma = \begin{cases} E\varepsilon & if\ \sigma < \\ \sigma^y + E_t\left(\varepsilon - \frac{\sigma^y}{E}\right) & if\ \sigma \geq \sigma^y \end{cases} \quad [1]$$

This model implies that the tensile stress (σ) can be discretized into two regions: an elastic region, where ε is the tensile strain and E is the elastic modulus; and a region of plastic deformation, where E_t is the tangent modulus and σ^y is the yield stress. This model is found to fit the experimental stress-strain curves reasonably well; fit is improved when the transition point between the two regions is empirically adjusted as follows:

$$\sigma = \begin{cases} E\varepsilon & if\ \sigma < a\sigma^y \\ \sigma^y + E_t\left(\varepsilon - \frac{\sigma^y}{E}\right) & if\ \sigma \geq a\sigma^y \end{cases} \quad [2]$$

where a is an empirical scaling factor (sample-dependent; $0.75 \leq a \leq 0.94$).

Using Equation 2, electrodes and bare current collectors have been computationally modeled (representative fits shown in Fig. 3). Of the parameters in Equation 2, the elastic modulus (E) is the most commonly reported material property, and thus is used as a comparative basis to probe the effects of both cycling-aging and strain rate on component tensile response. Fig. 4 compares the elastic moduli of fresh and C-A components; additionally, the moduli of cycled (but not calendar-aged) electrodes at one strain rate are included for comparison. As is shown, fresh, cycled, and C-A electrodes all show drastically reduced elastic moduli relative to their respective bare current collectors. The reported brittleness of current collectors in LIB cells[47] has been attributed to structural damage induced during manufacturing by the electrode calendaring processes.[46,47] The tensile response of the active material negligibly contributes to the overall electrode tensile response,[35,46] and thus the decrease in elastic moduli for fresh anode and cathode samples can be taken to approximately reflect the current collector damage caused by the coating of active material. No significant degradation is observed for either cycled or C-A anodes relative to fresh anodes. However, cathodes experience a statistically significant decrease in the elastic modulus with cycle-aging across all strain rates. Notably, this reduction in elastic modulus appears to occur during cycling as evidenced by a nearly identical elastic modulus for cycled and C-A cathodes at a strain rate of 0.0001 s^{-1}. This may be due to side reactions that occur during repeated cycling, which could increase the flexibility of the Al current collector matrix.

Strain rate is found to influence component tensile response, albeit irregularly. For bare current collectors, the elastic modulus is positively and logarithmically correlated with strain rate (Fig. 5a). For fresh electrodes and C-A anodes, there is variation but no clear correlation between elastic modulus and strain rate; C-A cathodes show a negative logarithmic correlation between elastic modulus and strain rate (Figs. 5b–5c). The loss of positive strain rate dependence in coated electrodes, relative to bare current collectors, supports the notion that the coating of active material permanently alters the current collector matrix.

The observed changes in electrode tensile behavior with cycle-aging has significant implications for the design of an R2R direct recycling process. Specifically, R2R processing requires precise control of tension: if tension is too low, sagging will occur; if tension is too high, the material will fracture.

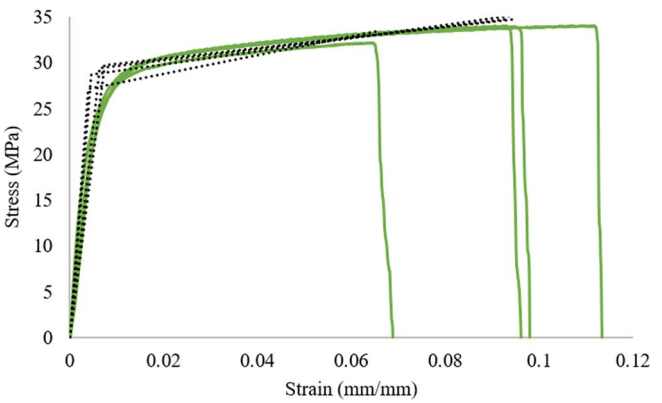

Figure 3. Anode tensile stress-strain response for a strain rate of 0.001 s^{-1}. Solid green lines indicated experimental data (four sample repeats); black dots indicate model curves regressed using Equation 2.

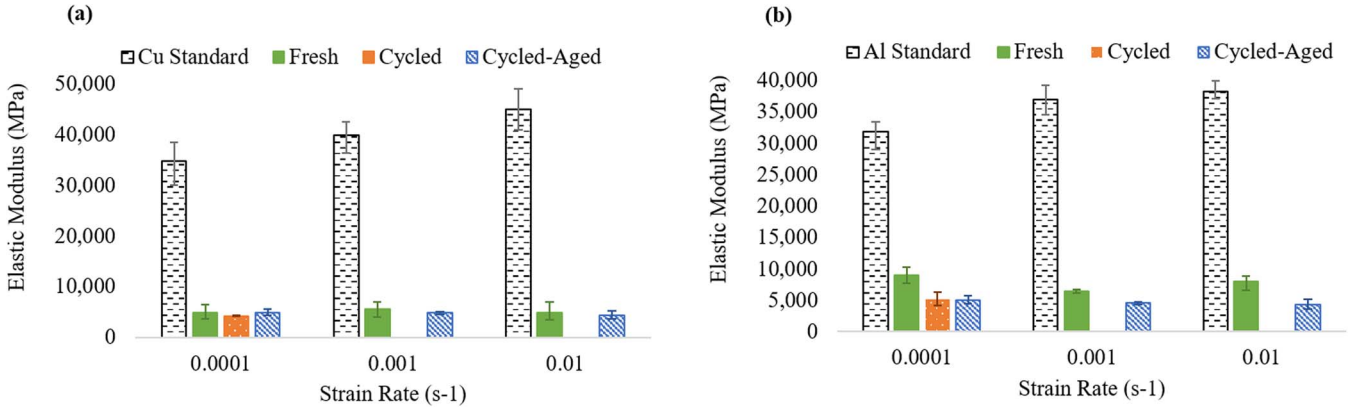

Figure 4. Elastic moduli for fresh, cycled, and C-A components and bare current collectors: (a) anode and (b) cathode. Error bars represent the range of elastic moduli calculated at each strain rate from six samples. The elastic modulus of cycled components was obtained at a strain rate of 0.00082 s^{-1} (data from Wu et al. (2017)).[32]

It has been suggested that the tension-dependent elastic strain in an R2R process can be modeled using Hooke's Law:[33]

$$T = AE\varepsilon \quad [3]$$

where A is the cross-sectional area; E is the elastic modulus; and ε is the tensile strain. Thus, for each component, a value of maximum allowable tension can be calculated from the experimental values of E and ε.

As shown in Fig. 6, the maximum tension C-A components can tolerate before undergoing irreversible mechanical damage (i.e., plastic deformation) is reduced relative to that of fresh components. In particular, the maximum tension tolerated by C-A anodes is between 35 and 317 N (14-59%) lower than the maximum tension tolerated by fresh anodes; for C-A cathodes, the maximum tension is reduced by 26 to 257 N (13-65%). This trend is especially evident at higher strain rates (0.01 mm/mm). However, for both anode and cathode, the values of maximum allowable tension for C-A electrodes are higher than for bare current collectors (at least 48 N higher for C-A anodes vs bare Cu, and at least 23 N higher for C-A cathodes vs bare Al). This implies that tension control parameters optimized for the coating of bare current collectors should not induce mechanical damage on end-of-life electrodes being processed in a R2R recycling line.

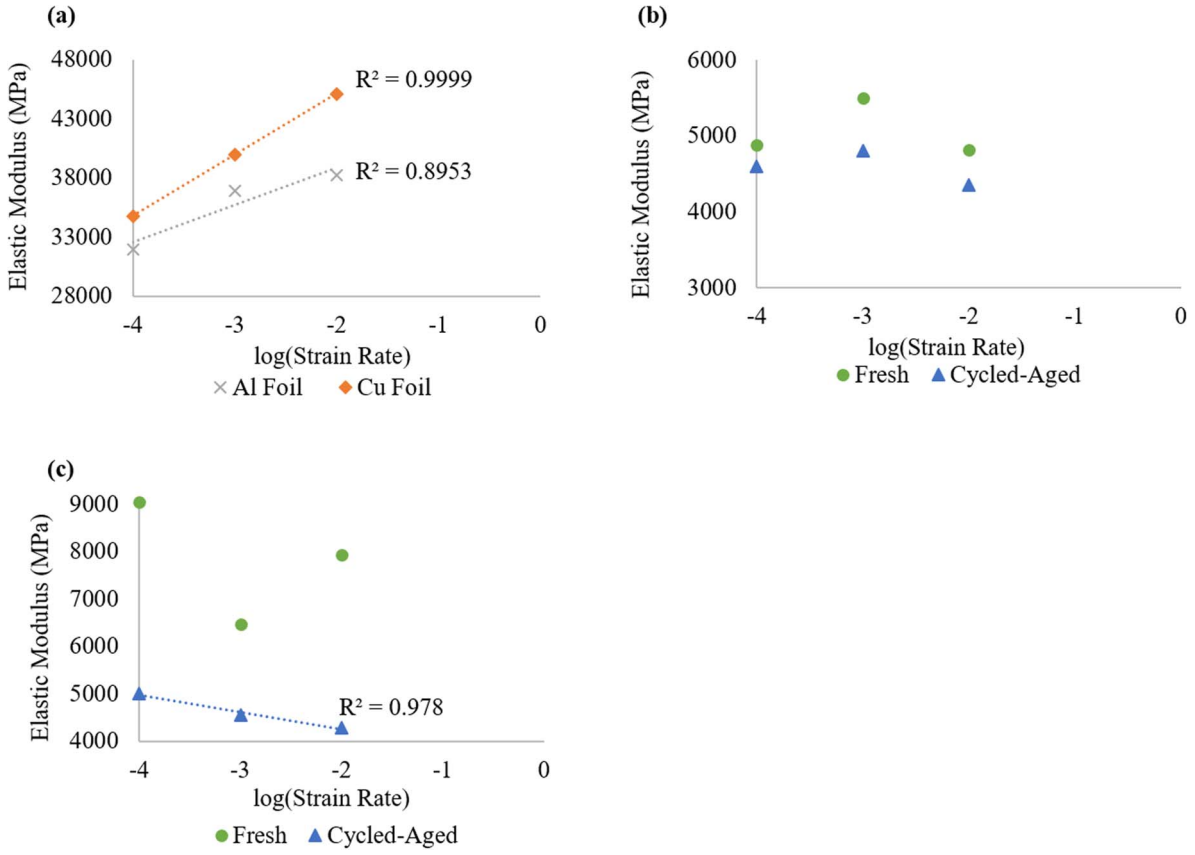

Figure 5. Strain rate dependence of (a) current collectors; (b) anodes; and (c) cathodes. Current collectors show positive logarithmic strain rate dependence and coated electrodes show no consistent strain rate dependence, with the exception of C-A cathodes (negative logarithmic strain rate dependence).

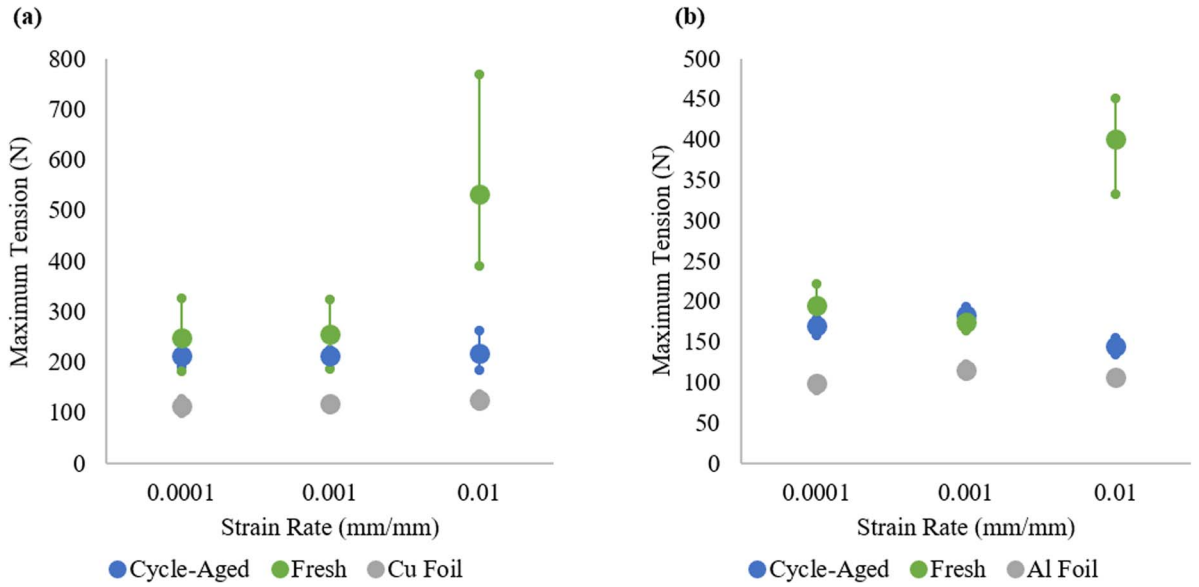

Figure 6. Maximum allowable tension before plastic deformation for (a) anode and Cu current collector and (b) cathode and Al current collector. Maximum allowable tension is calculated using Equation 3 with values of E and ε experimentally determined at each reported strain rate. Error bars represent the range of E and ε between sample repeats at the onset of plastic deformation.

It should be mentioned that material tension is only one of a multitude of complex parameters incorporated into the process control of R2R systems. The observed strain rate dependence of both current collectors and coated electrodes suggests that a more complex model of the R2R process, such as that proposed by Kang and Baumann[33] is warranted.

Compression

While direct recycling methods are still under development, it is possible that the process may include machine calendering to smooth the active material surface. Thus, determining the behavior of recycling feedstock materials under compressive loads is essential to the development of process engineering controls. The response of components to a uniform compressive load is shown in Fig. 7. Under our test conditions, compressive failure was not induced; this is in contrast to our earlier work, in which anode failure was observed at stresses as low as 150 MPa.[44] In-house testing has suggested that sample size and thickness strongly influences the occurrence of compressive failure, and due to instrument limitations, a single component layer cannot be effectively tested. Therefore, the lack of compressive failure in this analysis does not conclusively imply that compressive behavior can be neglected in recycling process design.

Despite the lack of ultimate failure, there is a difference in compressive response observed between fresh and C-A components. For anodes, C-A components show a decreased elastic modulus relative to fresh components. For cathodes, the contrast is more pronounced: C-A components show a distinct S-shaped compression curve, implying a transition to the plastic deformation stage. This transition occurs at a stress of 61–65 MPa for C-A cathodes, whereas fresh cathodes can withstand stresses of at least 75 MPa (test limit, based on the installed load cell) without undergoing plastic deformation. Thus, C-A cathodes experience irreversible mechanical damage at lower stresses than do their fresh counterparts. This behavior suggests that ultimate failure may also occur at lower stresses for C-A cathodes, as plastic deformation typically precedes failure.

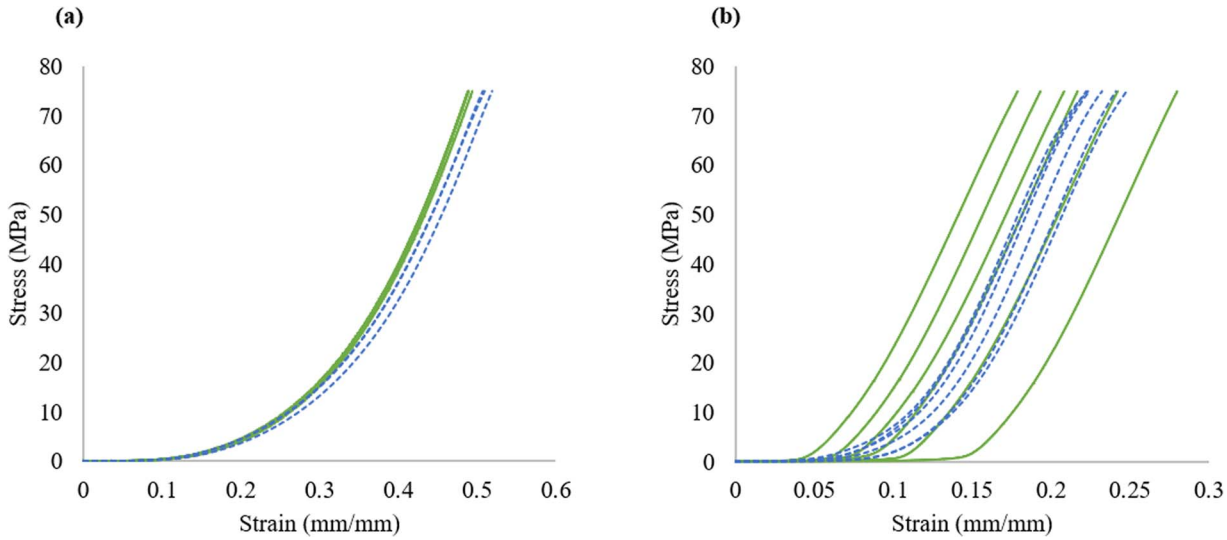

Figure 7. Experimental compressive stress-strain response for (a) anode and (b) cathode for a strain rate of 0.001 s^{-1}. Solid green lines indicate fresh samples; blue dashes indicate C-A samples.

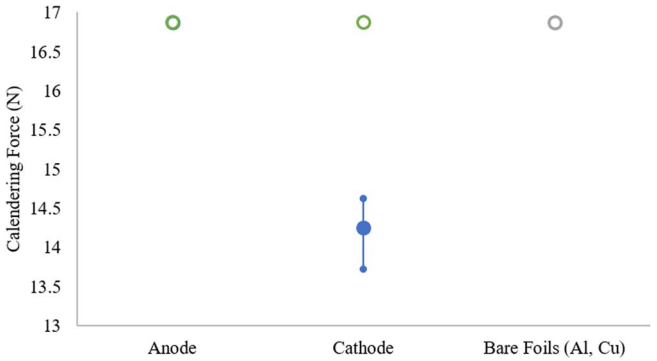

Figure 8. Maximum allowable calendering force before onset of plastic deformation, assuming a 75 mm wide electrode and a 3 m distance between rolls in an R2R system (as described by Urdampilleta et al. (2015)[37]). Open circles indicate samples that did not show plastic deformation within the scope of the present experimental analysis, and thus are expected to withstand calendaring forces above the indicated value. For C-A cathodes, error bars represent the range of measured stress values between sample repeats at the onset of plastic deformation.

Additionally, greater variability between sample replicates is observed for fresh cathodes than for C-A cathodes. Up to the test limit, fresh cathodes demonstrate elastic behavior (linear stress-strain relationship). In this elastic region, we anticipate the mechanical response of fresh cathodes to be governed by the polymeric binder and the presence of porosity, both of which are highly sensitive to mechanical load. The inhomogeneity of both binder distribution and porosity across fresh cathodes has been demonstrated,[48] and may explain the variability in compression response for replicates of fresh cathode samples. For C-A cathodes, we anticipate that electrolyte degradation products build up in the inter-particle pores (see "Electrochemical Cycling"). The filling of porous regions with degradation products may reduce the sensitivity of C-A cathodes to mechanical load, resulting in the observed reduction in variability between replicates.

The observed compressive response indicates that a calendaring step during the direct recycling process is unlikely to damage anodes (fresh or C-A) or fresh cathodes. However, based on typical dimensions of an 18650 cell and assuming a distance of 3 m between rolls,[49] C-A cathodes can only withstand a calendering force of approximately 14 N before the onset of irreversible mechanical damage (Fig. 8).

The importance of characterizing both the tensile and compressive responses of LIB components has already been established, as electrodes show different behaviors under each type of mechanical load.[46] The current analysis confirms this conclusion, particularly in the context of direct recycling methods, where feedstocks are expected to undergo both tensile and compressive stresses as they are refurbished.

Electrochemical Cycling

Understanding the mechanical behaviors of end-of-life electrodes is crucial to developing and controlling a R2R direct recycling process. However, such a physical approach is incomplete without consideration of the chemical and electrochemical processes driving the recycling methods. To this end, a variety of cycling tests have been conducted to identify the source and extent of electrochemical degradation that can be attributed to each component. This, in turn, helps to inform the aims and methods of the recycling process.

In order to assess the effects of C-A components on overall cell performance, a variety of full coin cells were assembled. In each of these cells, one component (anode or cathode) had been previously cycle-aged, while the remaining components were uncycled and had never been exposed to electrolyte. By isolating each component in this manner, individual contributions to the degradation of the cell's capacity can be identified and analyzed.

As shown in Fig. 9, the cycle-aging of anodes contributes most significantly to the whole cell performance; after 25 cycles, cells containing C-A anodes show ~93% reduction in capacity as compared to cells containing fresh components. Interestingly, the capacity of cells with C-A anodes and fresh cathodes is significantly lower than the capacity of cells with C-A anode and cathode. This may be a result of the mismatch in specific capacity between C-A anodes and fresh cathodes, which has previously been observed to be a dominant factor in overall cell capacity loss.[50] Such a shift in electrode balancing has been attributed to a loss of cyclable Li during both cycling and calendar aging,[50] and may also lead to ineffective Li^+ transfer upon initial charge and perhaps the onset of destructive surface side reactions.

For cells containing C-A cathodes, the effect on overall cell capacity degradation is much less (~21% capacity reduction after

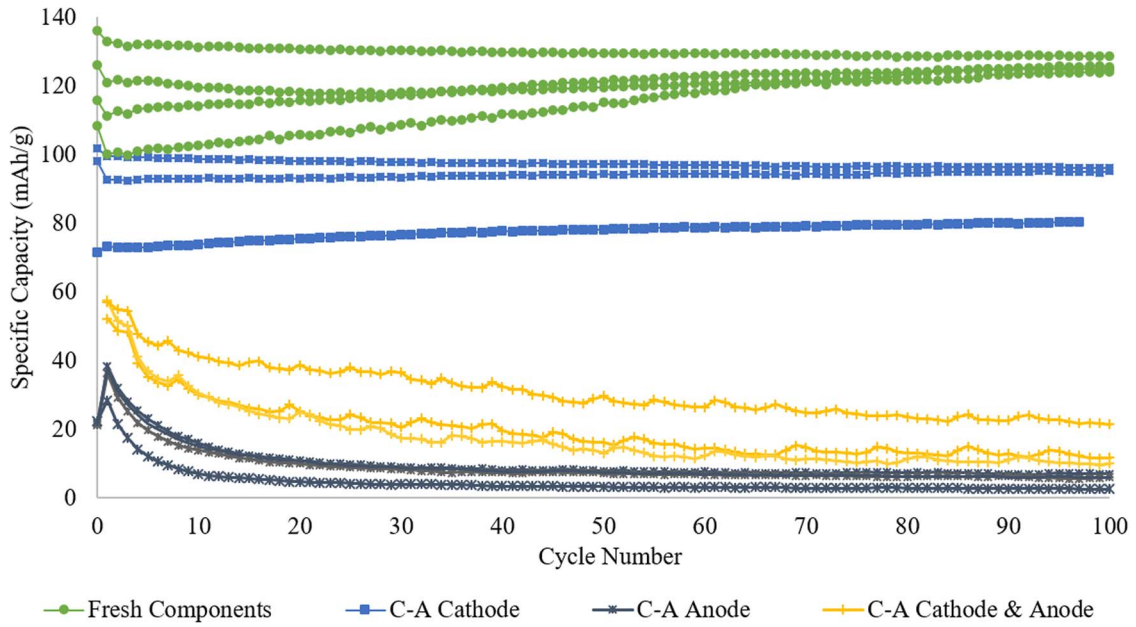

Figure 9. Specific capacity (mAh/g) of coin cells prepared with various combinations of fresh and C-A components over 100 cycles. Mass used for specific capacity determination is mass of cathode minus mass of current collector in each case.

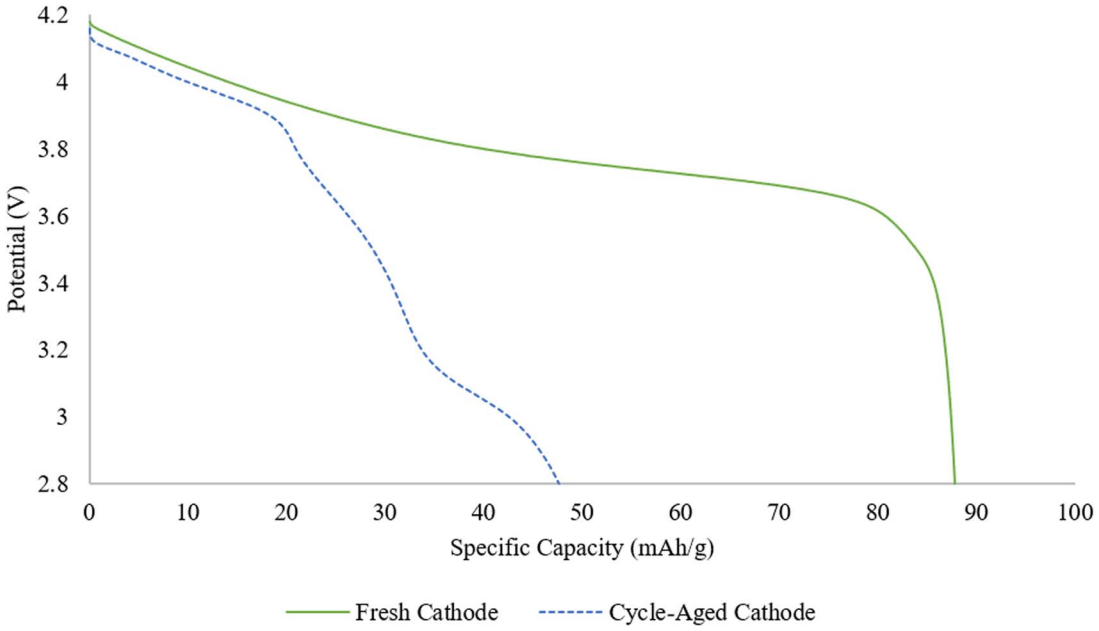

Figure 10. Discharge profiles of a representative cell containing a fresh cathode (solid green line) and a cell containing a C-A cathode (blue dashes), after 5 cycles.

25 cycles). Since cathodes are emerging as the primary target for direct recycling methods, the origin of this degradation was probed further. Half-cells containing either fresh or C-A cathodes were prepared and cycled vs Li metal to analyze changes in the cathodic reaction mechanism with cycling. The discharge profiles of these cells are shown in Fig. 10.

At low values of specific capacity (<1 mAh/g), both sets of cells (fresh cathodes, C-A cathodes) experience a sharp drop in potential; this is due to the resistance of the electrode materials and tends to occur between the end of the charge cycle and the beginning of the discharge cycle.[51] In the intermediate region of specific capacity (~10-85 mAh/g), a plateau is observed for fresh cathodes. This is consistent with favorable bulk diffusion in the electrolyte and a layered NMC structure. However, cells with C-A cathodes show much more significant decay in this region and are also found to demonstrate stepwise drops in voltage with increasing specific capacity. This indicates the presence of a spinel phase, suggesting degradation of the layered structure with cycle-aging. Finally, a sharp decrease in potential occurs at ~45 mAh/g for cells with C-A cathodes versus ~100 mAh/g for cells with fresh cathodes. This region corresponds to the diffusion of Li into the primary particle, implying that the specific capacity of C-A cathodes may be adversely affected by electrolyte buildup in the pores.

A corresponding dQ/dV plot is presented in Fig. 11. For cells with fresh cathodes, a peak at ~3.73 V is observed; this has been attributed to Li occupation within octahedral sites during the reduction of Ni and Co[52] and implies fast reaction kinetics, such that one singular reaction voltage is dominant. A shoulder at ~4.15 V is also apparent, which may be attributable to Li occupation within tetrahedral sites in the (delithiated) Li layer.[53] For cells with C-A cathodes, four separate peaks are observed, implying that kinetics have slowed and enabling

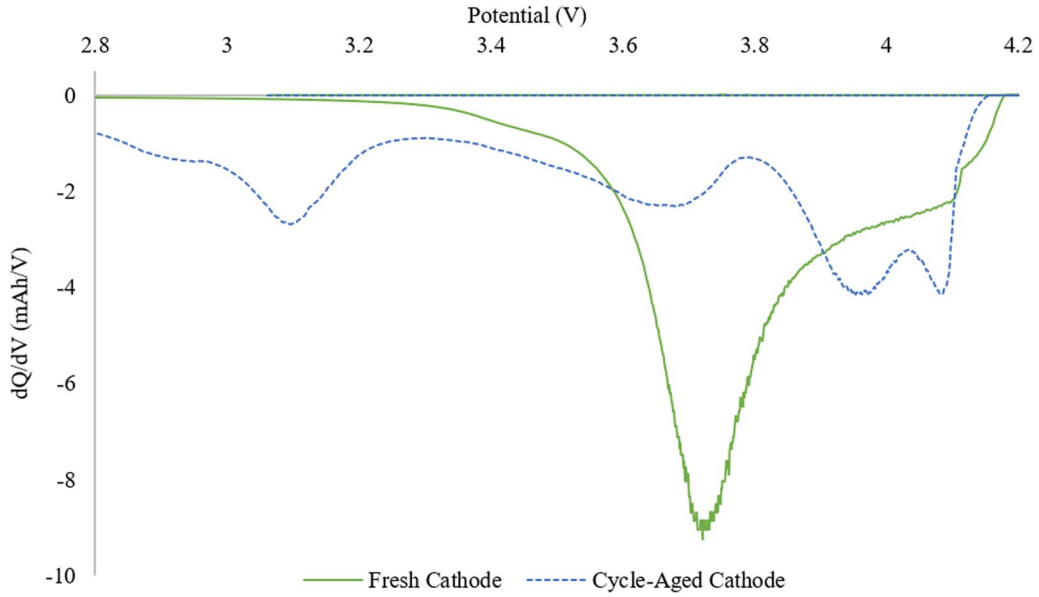

Figure 11. Differential discharge capacities (dQ/dV) of representative half-cells containing either fresh (solid green line) or C-A (blue dashes) cathode. Fifth discharge cycle is shown.

discernment of distinct reduction reactions. The three peaks at higher voltages (∼4.08 V, ∼3.97 V, and ∼3.68 V) are likely attributable to the reduction of Ni, Co, and Mn, respectively. The shoulder at ∼4.15 V is notably absent, indicating minimal Li occupation in tetrahedral sites and perhaps suggesting an overall decrease in cyclable Li. The emergence of the Mn peak and its increased contribution to overall discharge capacity with cathode cycling has been previously established[52] and is verified by this analysis. A general shift toward higher reaction potentials has been reported for cycled cathodes,[54] and may explain the observed deviation from the ideal reduction potentials of the transition metal species. The fourth peak, occurring below 3.15 V, may be related to redox reactions occurring in regions of the cathode that have undergone a phase change, such as to a surface spinel. This conclusion is supported by XRD measurements, which suggest the degradation of the layered NMC structure upon cycle-aging (see Fig. S3).

In a direct recycling process focusing on cathode remediation, the present electrochemical analysis offers several insights. Firstly, the absence of Li in tetrahedral sites upon discharge of C-A cathodes may suggest overall Li deficiency in the cathode. Such a reduction in the cyclable Li inventory has been identified as a primary cause of capacity fade with battery aging,[55,56] and may be due to both lithium plating during cycling[57] and the growth of passivation layers on the electrode surfaces. Thus, replenishing the source of cyclable Li will be crucial to the refurbishment of aged cathodes.[26–29] Secondly, there is strong evidence of structural degradation from layered to spinel structure which does not appear to be reversible via relithiation (i.e., half-cell cycling). The effects of this phase change on cathode performance in recycled cells should be explored further, and additional characterizations of C-A cathodes will be crucial to understanding the effects of structural degradation on electrochemical performance.

Conclusions

In this paper, we aim to provide a foundation for the development of industrial-scale direct recycling methods for LIBs. We investigate the mechanical properties of LIB components that have been cycled and calendar-aged (i.e., recycling inputs) to determine the feasibility of winding and calendering processes. Further, we determine the contribution of cathode cycle-aging to the overall electrochemical degradation of the cell and use electrochemical analysis to suggest several remediation strategies.

Cycle-aged electrodes show decreased yield strength and ultimate strength under tensile stress. This implies that the maximum tension C-A components can tolerate before the onset of irreversible damage is reduced relative to fresh components (by 14–59% for anodes and 13–65% for cathodes). Such insight can inform design control parameters for an R2R direct recycling process. Further, for bare current collectors, the elastic modulus shows a strong logarithmic correlation with strain rate; this strain rate dependence is largely lost for coated electrodes. This suggests that the coating process significantly alters the current collector matrix and may have implications for more complex recycling process control parameters.

Under our test conditions, compressive failure is not observed for any samples. However, C-A cathodes reach elastic deformation at lower stresses than their fresh counterparts, implying a reduction in compressive strength. Further testing is recommended to confirm electrode compressive response in the context of direct recycling, where a single electrode sheet will undergo calendering.

Finally, we report that anode cycle-aging dominates the overall loss of cell capacity in a full cell, but emphasize study of cathode degradation, as cathodes are currently the primary target for direct recycling schemes. Structural degradation (from layered to spinel phase) and the buildup of electrolyte residues at both the primary particle and the inter-particle pore space are proposed as dominant degradation mechanisms.

The mechanical and electrochemical findings of this analysis will inform the development of a specific testing/sorting protocol for LIB recycling feedstocks, with the goal of improving the feasibility of implementing novel direct recycling methods at the industrial scale.

Acknowledgments

This work was authored the National Renewable Energy Laboratory (NREL), operated by Alliance for Sustainable Energy, LLC, for the U.S. Department of Energy (DOE) under Contract No. DE-AC36-08GO28308. Funding provided by the U.S. DOE Vehicle Technologies Office (VTO) under the ReCell Center for Advanced Battery Recycling; program manager Samuel Gillard is gratefully acknowledged. This work was also supported in part by the U.S. Department of Energy, Office of Science, Office of Workforce Development for Teachers and Scientists (WDTS) under the Science Undergraduate Laboratory Internships Program (SULI). The views expressed in the article do not necessarily represent the views of the DOE or the U.S. Government. The U.S. Government retains and the publisher, by accepting the article for publication, acknowledges that the U.S. Government retains a nonexclusive, paid-up, irrevocable, worldwide license to publish or reproduce the published form of this work, or allow others to do so, for U.S. Government purposes.

ORCID

Kae Fink https://orcid.org/0000-0001-9363-4632
Shriram Santhanagopalan https://orcid.org/0000-0003-4703-1341
Lei Cao https://orcid.org/0000-0003-2899-5436

References

1. Z. M. Research, *GlobeNewswire News Room* (2018).
2. C. Curry, "Lithium-Ion Battery Costs and Market", *Bloomberg New Energy Finance* (2017).
3. T. Michaels, presentation, "Collection & Recycling Perspective", *Lithium-Ion Battery Recycling Workshop*, Argonne, IL (2016).
4. A. Boyden, V. K. Soo, and M. Doolan, *Procedia CIRP*, **48**, 183 (2016).
5. J. Dewulf, G. Van der Vorst, K. Denturck, H. Van Langenhove, W. Ghyoot, J. Tytgat, and K. Vandeputte, *Resources, Conservation and Recycling*, **54**, 229 (2010).
6. L. Gaines, *Sustainable Materials and Technologies*, **1–2**, 2 (2014).
7. L. Gaines, presentation, "Li-Ion Battery End-of-Life Issues", *Lithium-Ion Battery Recycling Workshop*, Argonne, IL (2016).
8. M. Chen, X. Ma, B. Chen, R. Arsenault, P. Karlson, N. Simon, and Y. Wang, *Joule*, **3**, 1 (2019).
9. R. Arsenault, K. Snyder, and T. Miller, presentation, "OEM Perspectives on Battery Recycling", *International Discussion on Lithium-Ion Battery Recycling*, Golden, CO (2018).
10. T. W. Ellis and A. H. Mirza, NIST (2017) https://www.nist.gov/sites/default/files/documents/2017/04/28/245_battery_recycling_defining_the_market.pdf.
11. Q. Dai, presentation, "China Perspective on Lithium-Ion Battery Recycling", *International Discussion on Lithium-Ion Battery Recycling*, Golden, CO (2018).
12. Y. T. Kim, presentation, "Lithium-Ion Battery Recycling Korea", *International Discussion on Lithium-Ion Battery Recycling*, Golden, CO (2018).
13. S. Rothermel, M. Winter, and S. Nowak, in *Recycling of Lithium-Ion Batteries: The LithoRec Way*, edited by A. Kwade and J. Diekmann (Springer, 2018).
14. J. Diekmann, C. Hanisch, L. Froböse, G. Schälicke, T. Loellhoeffel, A-S. Fölster, and A. Kwade, *Journal of the Electrochemical Society*, **164**(1), A6184 (2017).
15. Y. Wang, E. Gratz, J. Heelan, and Z. Zheng, presentation, "Cathode to Cathode Lithium Ion Battery Recycling," Abstract MA2016-03 **465**, *18th International Meeting on Lithium Batteries*, Chicago, IL (2016).
16. Y. Wang, presentation, "A Closed Loop Process for the End-of-Life Electric Vehicle Li-Ion Batteries," Abstract MA2018-01 **610**, *233rd Meeting of the Electrochemical Society*, Seattle, WA (2018).
17. M. Caffary, presentation, "Umicore Battery Recycling", *International Discussion on Lithium-Ion Battery Recycling*, Golden, CO (2018).
18. Kinsbursky Brothers Integrated Recycling Solutions, "Battery Recycling Workshop: General Overview", *Lithium-Ion Battery Recycling Workshop*, Argonne, IL (2016).
19. X. Chen, H. Ma, C. Luo, and T. Zhou, *Journal of Hazardous Materials*, **326**, 77 (2017).
20. H. Ku, Y. Jung, M. Jo, S. Park, S. Kim, D. Yang, K. Rhee, E.-M. An, J. Sohn, and K. Kwon, *Journal of Hazardous Materials*, **313**, 138 (2016).
21. Y. Yang, S. Xu, and Y. He, *Waste Management*, **64**, 219 (2017).
22. M. Slater, presentation, "Considerations in Development of Recycling Methods for Li-Ion Cells", *The Battery Show North America*, Novi, MI (2016).
23. S. E. Sloop, US8846225B2 (2014).
24. S. E. Sloop, US9287552B2 (2016).
25. J. Wang, S. Soukiazian, M. Verbrugge, H. Tataria, D. Coates, D. Hall, and P. Liu, *Journal of Power Sources*, **196**(14), 5966 (2011).
26. H. Wang and J. F. Whitacre, *Energy Technology*, **6**(12), 2429 (2018).
27. X. Li, A. Burrell, and C. Ban, presentation, "Recycling Spent Battery Cathode Materials Using Electrochemical Relithiation," Abstract MA2019-01 **313**, *235th Meeting of the Electrochemical Society*, Dallas, TX (2019).

28. J. Coyle, X. Li, S. Santhanagopalan, and A. Burrell, presentation, "Recycle of End-of-Life NMC 111 Cathodes by Electrochemical Relithiation," Abstract MA2019-02 **449**, *236th Meeting of the Electrochemical Society*, Atlanta, GA (2019).
29. A. Montoya and J. T. Vaughey, presentation, "Relithiation of Cathode Materials for the Recycling of Lithium-Ion Batteries," Abstract MA2019-02 **444**, *236th Meeting of the Electrochemical Society*, Atlanta, GA (2019).
30. H. Bae, S. M. Hwang, I. Seo, and Y. Kim, *Journal of the Electrochemical Society*, **163**(7), E199 (2016).
31. S. E. Sloop, J. E. Trevey, L. Gaines, M. M. Lerner, and W. Xu, *ECS Transactions*, **85**(13), 397 (2018).
32. H. Shin, R. Zhan, K. Dhindsa, L. Pan, and T. Han, presentation, "A Scalable Froth-Flotation Separation Process for Direct Recycling of Li-Ion Batteries and Its Technical Feasibility," Abstract MA2019-02 **445**, *236th Meeting of the Electrochemical Society*, Atlanta, GA (2019).
33. H. Kang and R. R. Baumann, *International Journal of Precision Engineering and Manufacturing*, **15**(10), 2109 (2014).
34. J. Park, K. Shin, and C. Lee, *International Journal of Precision Engineering and Manufacturing*, **17**(4), 537 (2016).
35. W.-J. Lai, M. Y. Ali, and J. Pan, *Journal of Power Sources*, **248**, 789 (2014).
36. J. Cannarella, X. Liu, C. Z. Leng, P. D. Sinko, G. Y. Gor, and C. B. Arnold, *Journal of the Electrochemical Society*, **161**(11), F3117 (2014).
37. J. Xu, B. Liu, L. Wang, and S. Shang, *Engineering Failure Analysis*, **53**, 97 (2015).
38. X. Jiang, H. Luo, Y. Xia, and Q. Zhou, *SAE International Journal of Materials and Manufacturing*, **9**(3), 614 (2016).
39. X. Zhang, E. Sahraei, and K. Wang, *Journal of Power Sources*, **327**, 693 (2016).
40. E. Sahraei, M. Kahn, J. Meier, and T. Wierzbicki, *RSC Advances*, **5**, 80369 (2015).
41. J. W. Braithwaite, *Journal of The Electrochemical Society*, **146**(2), 448 (1999).
42. C. Lin, A. Tang, H. Mu, W. Wang, and C. Wang, *Journal of Chemistry*, **2015**, 104673 (2015).
43. J. Park, W. Lu, and A. M. Sastry, *Journal of the Electrochemical Society*, **158**(2), A201 (2011).
44. Z. Wu, L. Cao, J. Hartig, and S. Santhanagopalan, *ECS Transactions*, 199 (2017).
45. Z. Wu, L. Cao, and S. Santhanagopalan, presentation, "Interactions between Electrochemical Cycling and Mechanical Response of Li-Ion Battery Components", *International Conference on Advanced Lithium Batteries for Automobile Applications (AABA-10)*, Chicago, IL (2017).
46. C. Zhang, J. Xu, L. Cao, Z. Wu, and S. Santhanagopalan, *Journal of Power Sources*, **357**, 126 (2017).
47. H. Luo, X. Jiang, Y. Xia, and Q. Zhou, V009T12A052 (2015).
48. S. R. Daemi, C. Tan, T. Volkenandt, S. J. Cooper, A. Palacios-Padros, J. Cookson, D. J. L. Brett, and P. Shearing, *ACS Applied Energy Materials*, **1**(8), 3702 (2018).
49. I. Urdampilleta, I. de Meatza, K. Ugarte, P. M. Schweizer, N. Loeffler, G.-T. Kim, and S. Passerini, GREENLION Project: Advanced Manufacturing Processes for Low Cost Greener Li-Ion Batteries, in *Electric Vehicle Batteries: Moving from Research toward Innovation*, E. Briec and B. Müller, Editors, pp. 45 (2015).
50. P. Keil, S. F. Schuster, J. Wilhelm, J. Travi, A. Hauser, R. C. Karl, and A. Jossen, *Journal of the Electrochemical Society*, **163**(9), A1872 (2016).
51. C. Liu, Z. G. Neale, and G. Cao, *Materials Today*, **19**(2), 109 (2016).
52. C. S. Johnson, N. Li, C. Lefief, J. T. Vaughey, and M. M. Thackeray, *Chemistry of Materials*, **20**(19), 6095 (2008).
53. B. Song, H. Liu, Z. Liu, P. Xiao, M. O. Lai, and L. Lu, *Scientific Reports*, **3**, 3094 (2013).
54. J. A. Gilbert, J. Bareño, T. Spila, S. E. Trask, D. J. Miller, B. J. Polzin, A. N. Jansen, and D. P. Abraham, *Journal of the Electrochemical Society*, **164**(1), A6054 (2017).
55. M. Dubarry, C. Truchot, B. Y. Liaw, K. Gering, S. Sazhin, D. Jamison, and C. Michelbacher, *Journal of Power Sources*, **196**(23), 10336 (2011).
56. Y. Gao, S. Yang, J. Jiang, C. Zhang, W. Zhang, and X. Zhou, *Journal of the Electrochemical Society*, **166**(8), A1623 (2019).
57. B. V. Ratnakumar and M. C. Smart, *ECS Transactions*, **25**(36), 241 (2010).